January - February 2020
ISSN: 0193-4120 Page No. 16455 - 16464

Numerical Approach for Boundary Layer Flow of Sutter by Fluid with Heat Generation or Absorption and Chemical Reaction

M. Sreedhar Babu [1], G. Ravi Sankar [2], V.Venkata Ramana[3]
[1,2,3]Department of Applied Mathematics, Y.V.University, Kadapa, A.P

Article Info
Volume 82
Page Number: 16455 - 16464
Publication Issue:
January-February 2020

Article History
***Article Received**: 18 May 2019*
***Revised**: 14 July 2019*
***Accepted**: 22 December 2019*
***Publication**: 28 February 2020*

Abstract

The article presented here, seeks to research the boundary layer flow of heat and mass transfer in a non - Newtonian fluid combined with the Cattaneo - Christov heat flux model with heat generation or absorption and chemical reaction. The combined method is abridged taping appropriate related keys and resolved mathematically by combining the shooting method with the Runge-Kutta of the fourth method. The purpose is to investigate heat transfer using a revised from of the Fourier legislation of heat conduction known as Cattaneo - Christov temperature flux model. The factors that impact major guidelines are considered. The calculated effects of speed, heat and focus information are shown through graphs. Significant results are the following: The shear stress of the wall structure shows reverses designs for shear thinning and shear thickening liquids. The temperature and the thermal boundary coating stiffness raises with upsurge in high temperature era or absorption.

Keywords:*Sutter by fluid, heat and mass transfer, heat generation or absorption, chemical reaction.*

I. INTRODUCTION

Because of hydrodynamic stream and heat move issues, the present significant stretch sheet has been finished because of its mechanical destinations and essential significance in different specialized procedures. It additionally influences the consideration at the guaranteed geothermal focuses where the one-dimensional upper layer is sent. Thus, speed is especially restricted. What's more, extending sheet or contact divider investigation is related with a few conspicuous building precautionary measures in the fields of metallurgy and biochemical designing procedures (copper wire drawing, solidifying, tinning, and so forth.). These safeguards influence unending strip or fiber cooling as they are drawn through a latent fluid. "The crane [1] examined the stream brought about by leaf development. Numerous specialists, for example, Gupta and Gupta [2], Chen and Char [3], Dutta et al. [4] Material area By tallying the impacts of lower heat and mass exchange examinations, we have arrived at the Crane Study [1], a few pros have considered various portrayals of the issue and accomplished parallel intimations. : (Ishak et al. [5-8], Boutros et al. [9], Mahapatra et al. [10], Pal [11, 12] and Aziz et al. [13]).

Also, numerous non-Newtonian liquids are standing out in organic, mechanical and designing exercises. The investigation of the rheological properties of non-Newtonian fluids is significant in light of the different employments of these liquids. "The Navier-Stokes constitutive examination isn't adequate to pass on the conduct of complex liquids, for example, oil, slowed down fluids, polymer blurs, fuel, paints, and so forth. As of late, the liquid model Sutter [14,15] has picked up significance because of its

Published by: The Mattingley Publishing Co., Inc.

TEST Engineering & Management

January - February 2020
ISSN: 0193-4120 Page No. 16455 - 16464

profoundly productive numerical development and capacity to control the pseudo-plastic and extension liquid stock. Gangadhar et al. They as of late broke down the impacts of synthetic responses and convection conditions on distracting hyperbolic fluids past a stable expanded surface. [16]. The heat move instrument causes dynamic undertakings, for example, reactor cooling, sedate attractive heading, temperature conduction in the tissue, and warm administration of the electrical plate. This framework is predominantly depicted by the customary high temperature conduction Fourier technique [17]. There are significant restrictions to evaluating essential boosts legitimately in all arrangements. Temperature plot Cattaneo [18] advanced the law of heat conduction by joining heat unwinding articulations that influence heat transformation as heat waves. Christov [19] joined Oldroyd's upper convection branch into the situation of the time branch and made an invariant portrayal of the web. His work incorporates "CataneoChristov heat motion model". Han et al. [20] considered the heat move of the circulation of Maxwell liquid skates in the light of the Cattaneo-Christov model. Mustafa [21] played out an investigation on the trading of Maxwell's upper convective fluid exchange. A few endeavors were likewise as of late made in [22, 23]. Gangadhar et al. [24] Cattaneo-Christov temperature stream hypothesis masterfully ventured to every part of the heat move of MHD Carreau liquid over a developing chamber. Gangadhar et al. [25] Thenanofluid on the stretch chamber was investigated with the high temperature stream Cattaneo-Christov hypothesis utilizing unearthly static technique. Azhar et al. [26] The stagnation current of the Sutterby fluid forced by the Cattaneo-Christov heat stream model was numerically tried.

In certain liquid applications, the impacts of heat age (source) or retention (sink) are significant. Comparable instances of studies managing these impacts have been referred to by creators, for example, "Qasim [27]. heatGangadhar et al. [28] are exothermic/absorptive, versatile suction/mixture, and gooey scattering impacts tried to assess the progression of nanofluid limit layer over extended surface.

Analysts fixated on the above endeavors concentrated on the procedure of heat and mass exchange by consolidating the Cattono-Christov warming stream model of non-Newtonian liquids with exotherm or ingestion and the aftereffects of concoction responses. The Sutterby fluid example was chosen to research shear diminishing, shear thickening, and rheological properties of Newtonian fluids. Late evaluations may help advance neuroscience temperature and mass exchange and modern research.

II. MATHEMATICAL FORMULATION

Consider a two-dimensional laminar limit layer of incompressible stream, a sutter that speaks to the age of the liquid, a stretchable surface with heat age or assimilation, and a first request compound response. "The heat move component is investigated through the hypothesis of heat stream from Cattaneo-Christov. The surface was seen as predictable with a stream limited to the plane $\bar{y}$ = 0 and y> 0. As appeared in Figure 1, the stream is created by a straight stretch of the surface that is influenced by the concurrent damping of two equivalent and inverse powers along the x-pivot. With the starting point fixed, the surface is expanded at speed u_w (x) = ax. When a> 0, the development interim yx is an arrange assessed along the extension plane, the temperature of the opening ecological liquid is consistent T, and the focal point of the natural liquid is steady C.

The solicitation to get the impact of temperature changes between the seat and the ecological liquid accepts that there is a temperature-subordinate heat source/sink in the stream district. In this revision we believe that the volumetric toll of heat generation, signified by $q^{m}\,[w.m^{-3}]$ should be $q^{m} = Q_0(\bar{T} - \bar{T}_\infty)$) for $\bar{T} \geq \bar{T}_\infty$ and equal to zero for $\bar{T} \leq \bar{T}_\infty$ where

Q_0(>0) is the heat generation andQ_0(<0) is the heat absorption factor (Vajravelu and Hadjinicolaou [29])."

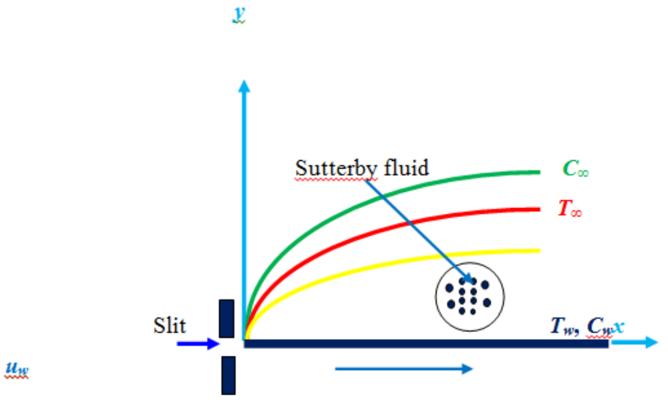

Fig. 1: Physical model and coordinate system

Without a weight angle, the administration condition that passes on mass, force, vitality, and preservation of species is given by:

$$\frac{\partial \bar u}{\partial \bar x} + \frac{\partial \bar v}{\partial \bar y} = 0 , \qquad (1)$$

$$\bar u \frac{\partial \bar u}{\partial \bar x} + \bar v \frac{\partial \bar u}{\partial \bar y} = \frac{\mu_0}{\rho}\frac{\partial}{\partial \bar y}\left[\frac{\partial \bar u}{\partial \bar y} + \frac{mB^2}{3}\left(\frac{\partial \bar u}{\partial \bar y}\right)^2\right],$$

(2)

$$\bar u \frac{\partial \bar T}{\partial \bar x} + \bar v \frac{\partial \bar T}{\partial \bar y} + \lambda_0 \left(\bar u \frac{\partial \bar u}{\partial \bar x}\frac{\partial \bar T}{\partial \bar x} + \bar v \frac{\partial \bar v}{\partial \bar y}\frac{\partial \bar T}{\partial \bar y} + \bar u \frac{\partial \bar v}{\partial \bar x}\frac{\partial \bar T}{\partial \bar y} + \bar v \frac{\partial \bar u}{\partial \bar y}\frac{\partial \bar T}{\partial \bar x} + \bar u^2 \frac{\partial^2 \bar T}{\partial \bar x^2} + \bar v^2 \frac{\partial^2 \bar T}{\partial \bar y^2} + 2\bar u \bar v \frac{\partial^2 \bar T}{\partial \bar x \partial \bar y}\right) = \alpha \frac{\partial^2 \bar T}{\partial \bar y^2} + \frac{Q_0}{\rho c_p}(\bar T - \bar T_\infty),$$

(3)

$$\bar u \frac{\partial \bar C}{\partial \bar x} + \bar v \frac{\partial \bar C}{\partial \bar y} = D\frac{\partial^2 \bar C}{\partial \bar y^2} - k_0(\bar C - \bar C_\infty),$$

(4)

Here $\bar u$ and $\bar v$ denote the velocity components along the $\bar x$ - and $\bar y$ - directions, respectively. $\upsilon = \mu_0 / \rho$ is the kinematic viscosity, μ_0 is the viscosity of the fluid, λ_0 is the fluid relaxation time, B is the material steady, m is the list of the force law. Here m> 0 compares to the shear thickness or enlarging liquid, m <0 speaks to the shear diminishing liquid or pseudoplastic liquid and for m = 0, the liquid is effectively a Newtonian liquid, $\bar T$ is the temperature of fluid, $Q_0(j s^{-1} m^{-3} K^{-1})$ is the dimensional heat generation $Q_0 > 0$ or absorption $Q_0 < 0$ factor, $\bar C$ is the concentration of fluid, ρ is the solidity of the fluid, c_p is the heat capacity of the fluid, k_0 is the chemical reaction rate coefficient and $\alpha = k / \rho c_p$ is thermal diffusivity, where k is the thermal conductivity.

The boundary conditions in the current problem are

$$\bar u = u_w(\bar x) = a\bar x,\ \bar v = 0,\ \bar T = \bar T_w,\ \bar C = \bar C_w, \quad \text{at} \quad \bar y = 0 \qquad (5)$$

$$\bar u \to 0,\ \bar T \to \bar T_\infty,\ \bar C \to \bar C_\infty, \ \text{as}\ \bar y \to \infty \qquad (6)$$

In the above equation, $\bar T_w$ is the temperature at the wall, and $\bar C_w$ is the temperature at the wall.

By using these transformations, we have

$$\eta = \sqrt{\frac{a}{v}}\bar y,\ \psi = \sqrt{va}\,\bar x\, f(\eta),\ \theta(\eta) = \frac{\bar T - \bar T_\infty}{\bar T_w - \bar T_\infty},$$

$$\phi(\eta) = \frac{\bar C - \bar C_\infty}{\bar C_w - \bar C_\infty}$$

(7)

In which ψ is the stream work, conditions (2) - (4) can be dense into a strategy for two customary differential conditions coupled as pursues:

Published by: The Mattingley Publishing Co., Inc.

TEST Engineering & Management

January - February 2020
ISSN: 0193-4120 Page No. 16455 - 16464

$$f'''(\eta) - f'^2(\eta) + f(\eta) f''(\eta) + \frac{m}{2} \mathrm{Re}\, De\, f''^2(\eta) f'''(\eta) = 0 \quad (8)$$

$$\frac{1}{\mathrm{Pr}} \theta''(\eta) + f(\eta)\theta'(\eta) - \gamma \left(f(\eta) f'(\eta)\theta'(\eta) + f^2(\eta)\theta''(\eta) \right) + Q\theta(\eta) = 0 \quad (9)$$

$$\frac{1}{Sc} \phi''(\eta) + f(\eta)\phi'(\eta) - Kr\phi(\eta) = 0 \quad (10)$$

Cousins represent the subsidiary regarding η. Prandtl's number is $\mathrm{Pr} = \upsilon / \alpha$, where α thermal diffusivity is. $De = B^2 a^2$ is the Deborah number, $\mathrm{Re} = \frac{a u_w(x)}{\upsilon}$ is the Reynolds number, $\gamma = \lambda_0 a$ is the non – dimensional thermal relaxation time, where a is a positive constant, λ_0 is fluid relaxation time, $Q = \frac{Q_0}{\rho a c_p}$ is the heat source or sink parameter, $Kr = \frac{k_0}{a}$ is the chemical reaction parameter, and $Sc = \upsilon / D$ is the Schmidt number. The boundary conditions for equations (6) and (7) are

$$f(\eta) = 0,\ f'(\eta) = 1,\quad \theta(\eta) = 1,\quad \phi(\eta) = 1, \text{ at } \eta = 0 \quad (11)$$

$$f'(\eta) \to 0,\quad \theta(\eta) \to 0,\quad \phi(\eta) \to 0, \text{ as } \eta \to \infty \quad (12)$$

The physical measure of intrigue is the coefficient of grinding of the skin C_f, which is characterized as

$$C_f = \frac{\tau_w}{\rho u_w^2}, \quad (13)$$

Or

$$-\mathrm{Re}_x^{1/2} C_f = \left[f''(0) + \frac{m}{6} De \mathrm{Re} \left(f''(0) \right)^3 \right]$$

Where $\mathrm{Re} = \frac{a\bar{x}^2}{\upsilon}$ is local Reynolds number based on the stretching velocity $u_w(\bar{x})$.

3.1 Solution procedures using the shooting method:

The mathematical process is used to resolve the differential technique Eqs. (8)-(10). This technique along with the boundary conditions Eqns. (11) - (12) is assimilated mathematically by implies of the Runge-Kutta method with systematic estimate of $f''(0), \theta'(0)$ and $\phi'(0)$ by the Newton-Raphson shooting technique until the boundary conditions at the immensity $f'(\infty), \theta(\infty)$ and $\phi'(\infty)$ degenerate exponentially to zero. In this method, it is fundamental to need a fitting limited an incentive for which the accompanying first request procedure is set up. Procedures for concentrating conditions (8)-(10) with limit conditions (11)- (12) into first-request customary differential conditions

$$y_1 = f,\ y_2 = f',\ y_3 = f'',\ y_4 = \theta,\ y_5 = \theta',$$
$$y_6 = \phi,\ y_7 = \phi'$$

$$y_3' = -\frac{1}{(1 + \frac{m}{2} \mathrm{Re}\, De\, y_3^2)} (y_1 y_5 - y_2^2),\ y_3(0) = \varepsilon_1$$

$$y_1(0) = 0,\ y_2(0) = 1,\ y_2(\infty) = 0$$

$$y_5' = -\frac{\mathrm{Pr}}{(1 - \gamma \mathrm{Pr}\, y_1^2)} (y_1 y_5 - \gamma y_1 y_2 y_5 + Q y_4),$$

$$y_5(0) = \varepsilon_2$$

$$y_4(0) = 1,\ y_4(\infty) = 0$$

$$y_7' = -Sc\, y_1 y_7 + Kr\, Sc\, y_6,\ y_7(0) = \varepsilon_3$$

$$y_6(0) = 1,\ y_6(\infty) = 0$$

The activating strategy includes evaluating $\varepsilon_1, \varepsilon_2$ and ε_3 by rehashing conditions up to the external limit. $y_2(\infty), y_4(\infty)$ and $y_6(\infty)$ are assured. The subsequent differential conditions can be

Published by: The Mattingley Publishing Co., Inc.

TEST Engineering & Management

January - February 2020
ISSN: 0193-4120 Page No. 16455 - 16464

consolidated utilizing the Runge-Kutta fourth request coordination plot. The above procedure is discussed until the outcomes are acquired up to the favored level of precision 10^{-6}. The point by point investigation is exhibited in the accompanying sections."

3.2 Validation of the Numerical Procedure:

For accreditation purposes, the outcomes were contrasted and information recently announced in the writing. Assessment of the investigation results is made in the present writing on these qualities of the roundabout example. These correlations are appeared in Furniture 1. The correlation was seen as in great concurrence with existing outcomes with less blunders.

IV. COMPUTATIONS AND DISCUSSION

The changed minute condition (8), vitality condition (9), and seed condition (10) subject to the limit states of conditions (11) and (12) were tackled numerically by the fourth-request strategy R-K. The count of the RK strategy was performed utilizing MATLAB. Numerical counts of Re, De, γ, Pr, Q, Kr, and Sc depicting the different qualities of as far as possible, for example stream, heat move, and mass properties are appeared and the outcomes are appeared in the table More illustrations. Also, table. In figs 2-10, the following data is generally utilized, (unless stated otherwise): Pr = 0.7,m = 0.5, De = Re = 0.3, Q = 0.2, γ = 0.2, Kr = 0.1 and Sc = 0.66.

For m <0, you can see the impact of shear diminishing. m = 0 is a Newtonian liquid, and for m> 0, the liquid speaks to shear thickening conduct. Figure 2 shows the impact of the associated force law register m on speed distribution. It tends to be seen that the speed dissemination increments with the gathered power type m. In this manner, the speed appropriation is higher for shear thickening liquids than for Newtonian and shear thickening liquids. In Figure 3, the speed appropriation is stamped when the Reynolds Re number qualities for the shear and shear weakening are extraordinary. From Figure 3a, it tends to be seen that when the Reynolds number is expanded on account of shear thickening (m> 0), the speed of the liquid is improved, though on account of a shear diminishing liquid, the benefit of Re (m <0) is expanded. it is clear. The power of the elastic is decreased and the liquid stream brakes as a preferred position (see Figure 3b). Liquid stream qualities are assessed by the Deborade number under explicit stream conditions. Deborade numbers for m> 0 and m <0 have very various consequences for liquid speed. Liquid stream is quickened as De builds (see Figure 4a), yet is hindered by the advantages of Deborah numbers dependent on the cutting liquid (see Figure 4b). The presence of De fills in as an undertaking in the extension of variable effect. This controls the creating liquid stream to grow the liquid, however the contrary side of the pseudoplastic liquid is watched. Figure 5 shows the stock of the power law record m in three groups: temperature forms with m <0, m = 0 and m <0. For shear diminishing liquids assessed in the other two sets, pursue the primary temperature. Figures 6 and 7 show the impact of the Reynolds Re number and the Deborah De number on the temperature dissemination. As can be seen from these figures, the thickness of the warm limit layer diminishes as the Reynolds Re number and the Deborah De number increment. Based on fluid expansion, De and Re surges generate elastic and viscous forces separately and control the improvement of the viscous boundary layer. This reduces the thermal boundary layer. Figure 8 shows the benefits of thermal recreation time and heat generation (Q> 0) or absorption (Q <0) in relation to temperature distribution. Plainly temperature scattering and warm limit layer thickness decline with outrageous warm unwinding time rates however increment with expanding Q. Heat from the sheet to the liquid. In this manner, liquid temperature diminishes with expanding warm unwinding parameter. Then again, the temperature field increments with diminishing heat retention. Once more, such highlights reach out a long way from the divider. The warm limit layer creates vitality and starts a temperature bend that

Published by: The Mattingley Publishing Co., Inc.

TEST Engineering & Management
January - February 2020
ISSN: 0193-4120 Page No. 16455 - 16464

happens at an expanding pace of Q> 0, yet when Q <0, the limit assimilates vitality and causes temperature. As the Q esteem diminishes, it diminishes extensively. Practically speaking, heat transport is improved or lessened by the inside age or assimilation of heat. The heat source can give a bigger warm dispersion layer, which can build the thickness of the warm limit layer, and then again diminish the thickness of the warm limit layer for heat ingestion.

Figure 9 shows that including the PrandtlPr figure slowly diminishes the temperature profile and lessens the warm limit layer thickness. The outrageous number of prandtls worth investigating, Pr> 1, is a case of a non-Newtonian polymer liquid. Prandtl number orders the remainder between the diffusivity of movement and the warm diffusivity. The most elevated Prandtl number is joined with a short warm diffusivity. What's more, the quantity of Prandtl is conversely corresponding to the warm conductivity. The polymer has a short warm conductivity and has an outrageous Prandtl number, for example, fluid metal. As the quantity of prandtls builds, the warm conductivity diminishes and the temperature of the limit layer diminishes essentially. Figure 10 shows the impact of the force law parameter m on the center dissemination. It very well may be considered that to be m grows the strong fluid properties decline. Figures 11 and 12 shows that the limit layer fixation diminishes with expanding Reynolds and Deborah numbers.

Figure 13 shows the focus profile reaction utilizing substance response parameters (Kr) and Schmitt number (Sc). Figure 13 shows that expanding the concoction response parameter (Kr) influence a stamped abatement in the fixation profile. The response term in the boundless layer of dimensionless focus (14), ie, - Kr □ , depends on the principal request irreversible substance response seen in both the liquid weight (uniform) and the divider. Albeit substance responses are chiefly diminished to two kinds, either homogeneous or heterogeneous, the previous is worry in momentum investigate. A uniform chemical reaction produces even dirt on the stationary part and uses the effects associated with the internal heat generation base. A negative mode of homogeneous chemical reaction was presented. Expanding the substance response parameter (Kr) will back off. Hence, because of the outrageous impacts of concoction responses, the thickness of the beat limits layer increments fundamentally. When chemical reactions occur, it is observed that the shared concentration decreases. In fact, if harmful, a chemical reaction occurs and the first class gradually disperses in the polymer viscoelastic fluid. This, in turn, faces a decrease in concentration magnitude and suppresses a permanent type of molecular diffusion that reduces the concentration of boundary layer thickness. Figure 13 shows that adding a Schmidt number (Sc) significantly reduces the magnitude of the concentration.

The Schmitt number is the proportion of the beat to the mass diffusivity, i.e., Sc = υ/D. The Schmidt number tallies the virtual utility of force and mass vehicle because of dissemination in the hydrodynamic limit layer (speed) and focus (species). When Sc> 1, the drive dissemination number surpasses the seed diffusion rate inverse worry for Sc<1.at the point when Sc = 1, the energy and fixation limit layer (seed) is a similar thickness and the diffusivity is the equivalent. In this way, the seed profile (fixation) bit by bit diminishes as the quantity of Schmidts increments. For gigantic Sc merits, there is a little cautioning legitimacy that compares to the rise of diffusibility of compound atoms, and the other way around.

Figure 14 shows the adjustments in the Deborade number and Reynolds Re number in the skin contact coefficient. This shows the coefficient of rubbing of the skin happens as the quantity of Deborah and Deborah increments. Reynolds Figures 15 and 16 show separate charts of skin grating against Deborah number for thickening and diminishing liquids. On

TEST Engineering & Management

January - February 2020
ISSN: 0193-4120 Page No. 16455 - 16464

the off chance that m> 0, the skin rubbing diminishes as the Deborah number increments, and the switch conduct of m <0 is portrayed.

V. CONCLUSION:

The motivation behind this article was to consider the heat and mass exchange of Sutter by liquids utilizing the Cattaneo-Christov heat stream model and exotherm or ingestion, and essential compound responses. A scientific answer for the issue of 2D stream towards the stretch sheet was performed by conjuring the calculation in the wake of utilizing association assessment. Suitable numerical impacts up to 6 digits have been accomplished. The principle discoveries of the present appraisal are: When the Reynolds Re and Deborah De quantities of a shear-thickening liquid happen, a speed field is made while the temperature and focus profiles are diminishing. New qualities for Pr and γ control the decline in temperature profile and warm limit layer thickness. Warm limit layer temperature and thickness happen with expanding heat age or retention. On account of shear thickening liquid, the numerical estimation of skin rubbing is diminished by enormous Re while it happens on account of shear diminishing. Ebb and flow explanatory new arrangements are helpful for scholarly research in the territories of heat and mass exchange and industry.

"Table 1 Contrast of local Nusseltnumber with the existing scores in literature for unlike worths of Pr in the case of Newtonian fluid

Pr	$-\theta'(0)$						
	Wang [30]	Gorla and Sidawi [31]	Khan and Pop [32]	Malik et al. [33]	Siri et al.[34] HWQM	Siri et al. [34] RK Gill	Present results
0.7	0.4539	0.5349	0.4539	0.45392	0.453930	0.453917	0.454447
2	0.9114	0.9114	0.9113	0.91135	0.911345	0.911358	0.911353
7	1.8954	1.8905	1.8954	1.89543	1.895489	1.895403	1.895400
20	3.3539	3.3539	3.3539	3.35395	3.353905	3.353904	3.353902

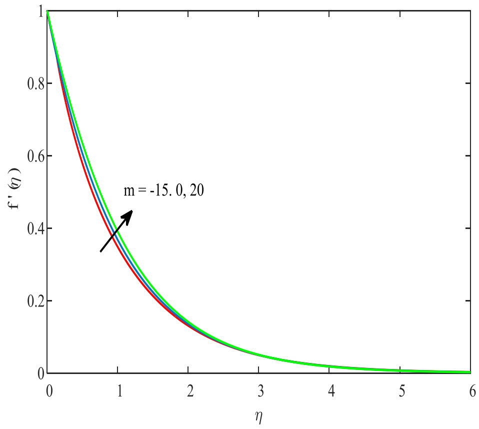

Fig. 2: Velocity distribution $f'(\eta)$ for different values of *m*.

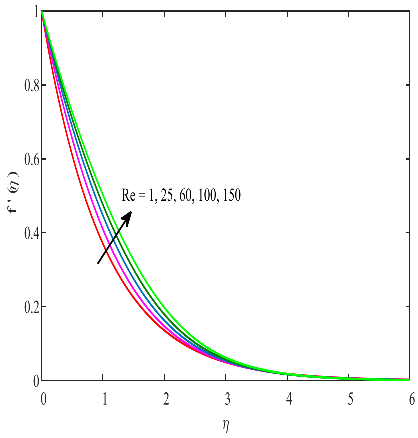

Fig. 3a: Velocity distribution $f'(\eta)$ for different values of *Re*for *m*> 0.

Published by: The Mattingley Publishing Co., Inc.

January - February 2020
ISSN: 0193-4120 Page No. 16455 - 16464

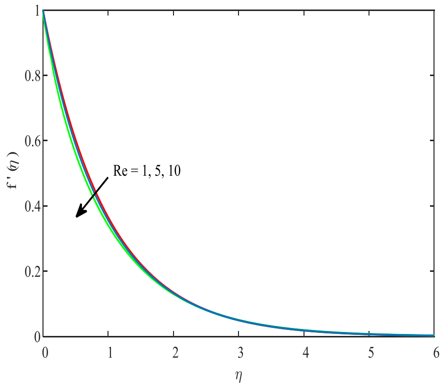

Fig. 3b: Velocity distribution $f'(\eta)$ for different values of *Re*for *m*< 0

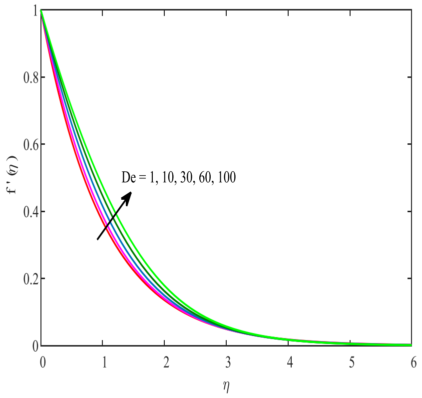

Fig. 4a: Velocity distribution $f'(\eta)$ for different values of *De*for *m*> 0.

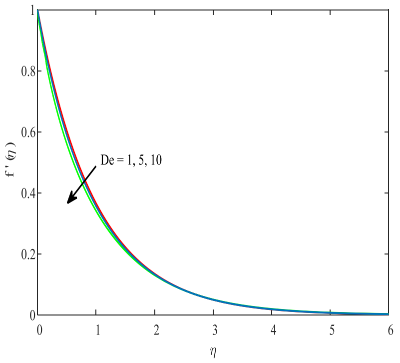

Fig. 4b: Velocity distribution $f'(\eta)$ for different values of *De*for *m*< 0.

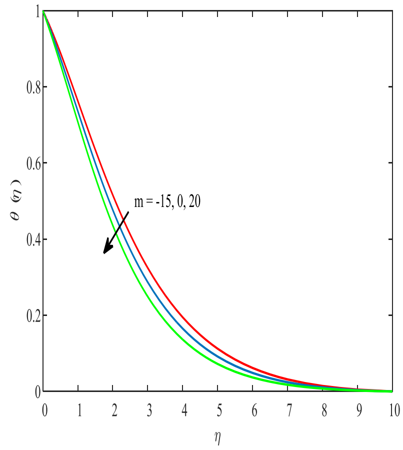

Fig. 5: Temperature distribution $\theta(\eta)$ for different values of *m*.

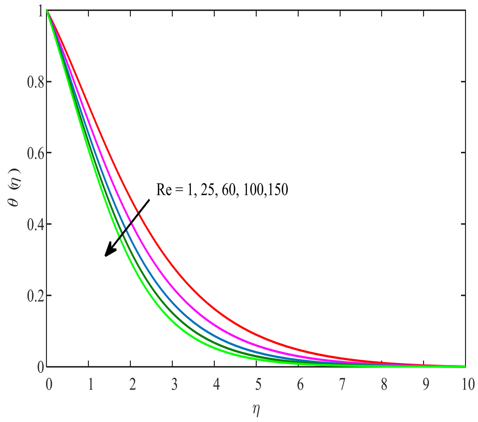

Fig. 6: Temperature distribution $\theta(\eta)$ for different values of *Re.*

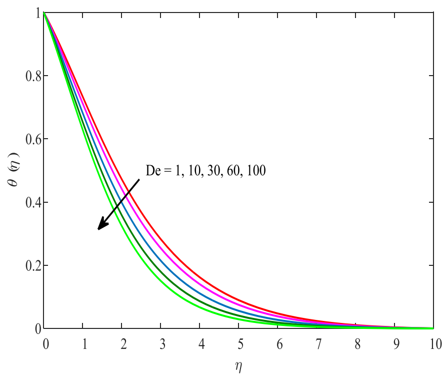

Fig. 7: Temperature distribution $\theta(\eta)$ for different values of *De*.

Published by: The Mattingley Publishing Co., Inc.

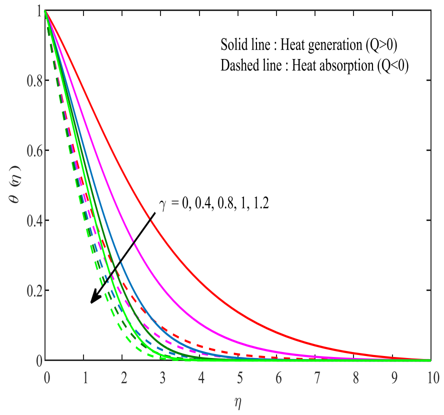

Fig. 8: Temperature distribution $\theta(\eta)$ for different values of γ and *Q*.

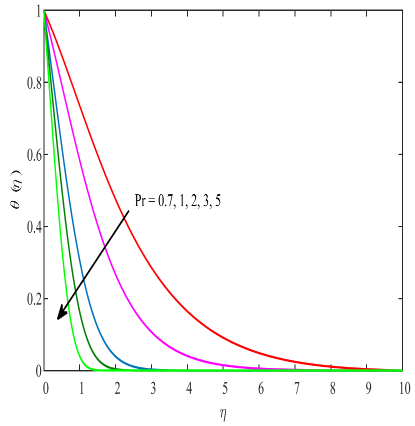

Fig. 9: Temperature distribution $\theta(\eta)$ for different values of *Pr*.

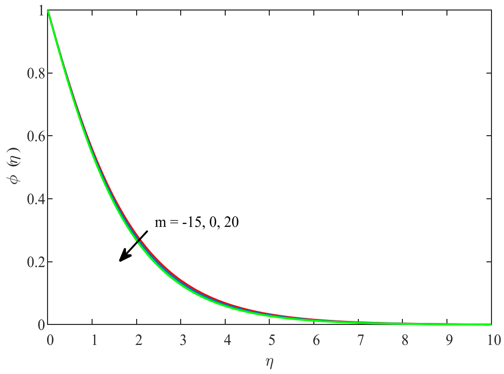

Fig. 10: Concentration distribution $\phi(\eta)$ for different values of *m*.

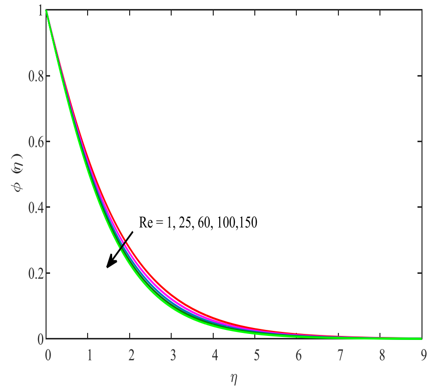

Fig. 11: Concentration distribution $\phi(\eta)$ for different values of *Re*.

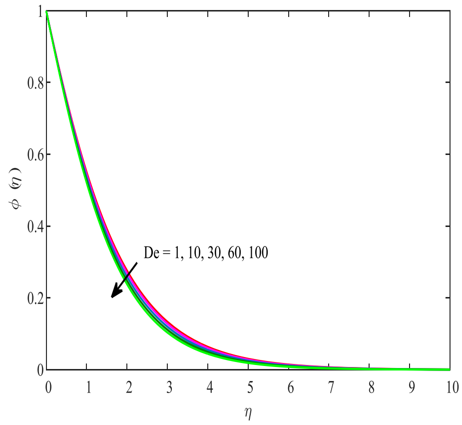

Fig. 12: Concentration distribution $\phi(\eta)$ for different values of *De*.

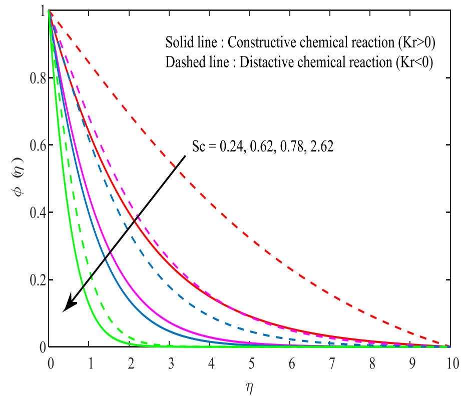

Fig. 13: Concentration distribution $\phi(\eta)$ for different values of *Sc* and *Kr*.

January - February 2020
ISSN: 0193-4120 Page No. 16455 - 16464

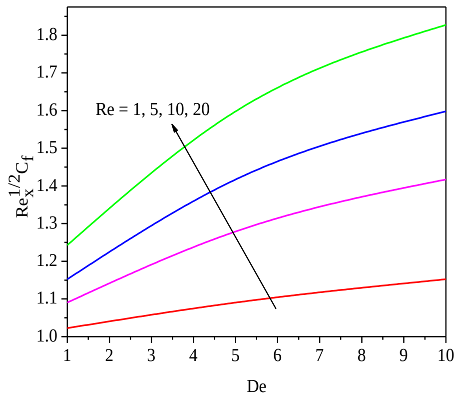

Fig. 14: Skin friction coefficient $Re_x^{1/2} C_f$ for different values of *De*and*Re*.

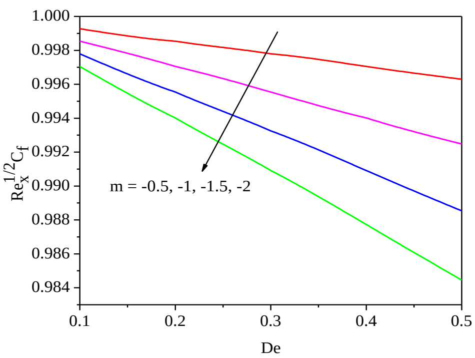

Fig. 15: Skin friction coefficient $Re_x^{1/2} C_f$ for different values of *De* and *m<0*.

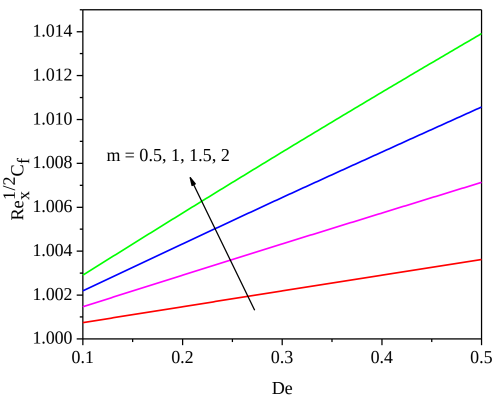

Fig. 16: Skin friction co-efficient $Re_x^{1/2} C_f$ for different values of *De* and *m*> 0."

REFERENCES

1. Flow past a stretching plate, Z Angew Math Phys, 21 (1970) 645-647 by Crane L.J.
2. Heat and mass exchange on an extending sheet with suction or blowing, Can J Chem Eng.,55 (1977) 744-746 by P. S. Gupta and A. S. Gupta.
3. Heat move of a ceaseless extending surface with suction or blowing, J Math Anal Appl., 135 (1988) 568-580 by C. K. Chen and M. I. Char.
4. Temperature field in the flow over a stretching sheet with uniform heat flux, IntCommun Heat Mass Transf., 12 (1985) 89-94 by B. K. Datta, P. Roy and A. S. Gupta.
5. Blended convection limit layers in the stagnation-guide stream to an extending vertical sheet, Meccanica, 41 (2006) 509-518 by A. Ishak, R. Nazar and I. Pop.
6. C.I. Christov, On outline apathetic detailing of the Maxwell-Cattaneo model of limited speed heat conduction, Mech. Res. Commun., 36(4) (2009) 481-486.
7. S. Han, L. Zheng, C. Li andX. Zhang, Coupled flow and heat transfer in viscoelastic fluid with Cattaneo-Christov heat flux model, Appl.Math. Lett.,38 (2014) 87-93.
8. M. Mustafa, Cattaneo-Christov heat flux model for rotating flow and heat transfer of upper convected Maxwell fluid, AIP Adv.,5 (2015) 047109.
9. Z. Iqbal, E. Azhar, E. N. Maraj and B. Ahmad, Impact of Cattaneo-Christov heat transition model on MHD hyperbolic digression liquid over a moving permeable surface, Front. Heat Mass Transf.,8 (2017) 25.
10. B. Ahmad and Z. Iqbal, An impact of Cattaneo - Christov heat transition model for Eyring Powell liquid over an exponentially extending sheet, Front. Heat Mass Transf.,8, 22 (2017)
11. K. Gangadhar, K.V. Ramana, O.D. Makinde and B.R. Kumar, MHD Flow of a Carreau Fluid Past a Stretching Cylinder with Cattaneo-Christov Heat Flux Using Spectral Relaxation Method, Defect and Diffusion Forum, 387 (2018) 91-105.

Published by: The Mattingley Publishing Co., Inc.